



Synthesis and biological evaluation of 2-substituted-4-(3',4',5'-trimethoxyphenyl)-5-aryl thiazoles as anticancer agents

Romeo Romagnoli^{a,*}, Pier Giovanni Baraldi^{a,*}, Maria Kimatrai Salvador^a, M. Encarnacion Camacho^a, Delia Preti^a, Mojgan Aghazadeh Tabrizi^a, Marcella Bassetto^b, Andrea Brancale^b, Ernest Hamel^c, Roberta Bortolozzi^d, Giuseppe Basso^d, Giampietro Viola^{d,*}

^aDipartimento di Scienze Farmaceutiche, Via Fossato di Mortara 17-19, Università di Ferrara, 44121 Ferrara, Italy

^bSchool of Pharmacy and Pharmaceutical Sciences, Cardiff University, King Edward VII Avenue, Cardiff CF10 3NB, UK

^cScreening Technologies Branch, Developmental Therapeutics Program, Division of Cancer Treatment and Diagnosis, National Cancer Institute, Frederick National Laboratory for Cancer Research, National Institutes of Health, Frederick, MD 21702, USA

^dDipartimento di Salute della Donna e del Bambino, Laboratorio di Oncoematologia, Università di Padova, 35131 Padova, Italy

ARTICLE INFO

Article history:

Received 2 July 2012

Revised 28 September 2012

Accepted 2 October 2012

Available online 12 October 2012

Keywords:

Tubulin

Thiazole

Combretastatin-A4

Colchicine site

Apoptosis

ABSTRACT

Antitumor agents that bind to tubulin and disrupt microtubule dynamics have attracted considerable attention in the last few years. To extend our knowledge of the thiazole ring as a suitable mimic for the *cis*-olefin present in combretastatin A-4, we fixed the 3,4,5-trimethoxyphenyl at the C4-position of the thiazole core. We found that the substituents at the C2- and C5-positions had a profound effect on antiproliferative activity. Comparing compounds with the same substituents at the C5-position of the thiazole ring, the moiety at the C2-position influenced antiproliferative activities, with the order of potency being $\text{NHCH}_3 > \text{Me} \gg \text{N}(\text{CH}_3)_2$. The *N*-methylamino substituent significantly improved antiproliferative activity on MCF-7 cells with respect to C2-amino counterparts. Increasing steric bulk at the C2-position from *N*-methylamino to *N,N*-dimethylamino caused a 1–2 log decrease in activity. The 2-*N*-methylamino thiazole derivatives **3b**, **3d** and **3e** were the most active compounds as antiproliferative agents, with IC_{50} values from low micromolar to single digit nanomolar, and, in addition, they are also active on multidrug-resistant cell lines over-expressing P-glycoprotein. Antiproliferative activity was probably caused by the compounds binding to the colchicine site of tubulin polymerization and disrupting microtubule dynamics. Moreover, the most active compound **3e** induced apoptosis through the activation of caspase-2, -3 and -8, but **3e** did not cause mitochondrial depolarization.

© 2012 Elsevier Ltd. All rights reserved.

1. Introduction

Microtubules are key components of the cytoskeleton and are involved in a wide range of critical cellular functions, such as cell division, where they are responsible for mitotic spindle formation and proper chromosomal separation.¹ Antimitotic agents are one of the main class of cytotoxic drugs for cancer treatment, and tubulin represents a known target for numerous small natural and synthetic molecules that inhibit the formation of the mitotic spindle.^{2,3} Combretastatin A-4 (CA-4, **1a**; Chart 1) isolated from the bark of the South African tree *Combretum caffrum*,⁴ is one of the well-known natural molecules that inhibits the spindle formation through its interaction with tubulin at the colchicine site.⁵ CA-4

inhibits cell growth at nanomolar concentrations, exhibiting inhibitory effects even on multidrug resistant cancer cell lines.⁶ The disodium phosphate prodrug of CA-4, named CA-4P (**1b**),⁷ has been prepared as a water-soluble derivative, and there have been promising results with **1b** as a tumor vascular disrupting agent in phase II clinical trials.⁸

Structure–activity relationship (SAR) studies of CA-4 have underlined that the presence of the 3,4,5-trimethoxy substituted A-ring and the 4-methoxy substituted B-ring separated by a double-bond with *cis*-configuration are fundamental for optimal antiproliferative activity.⁹ It has also been reported that 3-hydroxy group on the B-ring is not necessary for potent activity.¹⁰ The activity of CA-4 is hampered by isomerization of the active *cis*-stibene configuration into the corresponding inactive *trans* analogue. Replacement of the olefinic bond with a five-membered heterocyclic ring permitted retention of the correct geometric orientation of the two phenyl rings of CA-4, placing them at an appropriate distance for efficient interaction with the colchicine site of tubulin.¹¹

* Corresponding authors. Tel.: +39 0 532455303; fax: +39 0 532455953 (R.R.); tel.: +39 0 532455293; fax: +39 0 532455953 (P.G.B.); tel.: +39 0 498211451; fax: +39 0 498211462 (G.V.).

E-mail addresses: rromagnoli@unife.it (R. Romagnoli), baraldi@unife.it (P.G. Baraldi), giampietro.viola1@unipd.it (G. Viola).

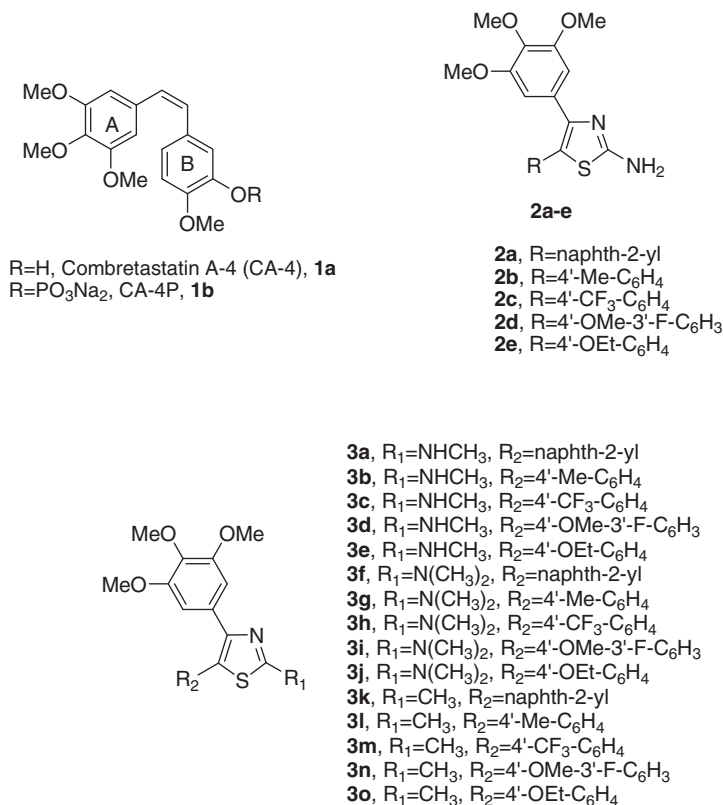


Chart 1. Lead structures of tubulin polymerization inhibitors

In our previous study, we reported the biological evaluation of a series of 2-amino-4,5-diarylthiazoles with general structure **2**, with the 2-aminothiazole moiety retaining the *cis*-olefin configuration of CA-4, with the 3',4',5'-trimethoxyphenyl ring of CA-4 at the C4-position of the thiazole ring.¹² On the basis of in vitro antiproliferative activity data, the best substituents for the C5-position of the thiazole ring, corresponding to the B-ring of CA-4, were a naphth-2-yl (**2a**) or a phenyl substituted at its *para*-position with a Me (**2b**), CF₃ (**2c**), MeO (**2d**) and EtO (**2e**) moiety.

Taking into consideration these results, in the present study we have synthesized a new series of analogues with general structure **3**, all of which retain at the C4- and C5-positions of the thiazole ring the same substituents as derivatives **2a–e**, examining the effect on biological activity derived by replacement of the amino group at the C2-position of the thiazole nucleus with different moieties, such as *N*-methylamine (**3a–e**), *N,N*-dimethylamine (**3f–j**) and methyl (**3k–o**).

2. Chemistry

2-Substituted-4-(3',4',5'-trimethoxyphenyl)-5-aryl thiazole derivatives with general structure **3** were prepared following the reaction sequence shown in Scheme 1. 4-Substituted thiazoles **6a** and **6c** were formed by condensation of 2-bromo-1-(3',4',5'-trimethoxyphenyl)ethanone **4** with *N*-methylthiourea or thioacetamide, respectively, in refluxing ethanol. The former compound **6a** was transformed into the corresponding *N*-acetyl analogue **6d** by treatment with a refluxing mixture of acetic anhydride and sodium acetate. The 2-*N,N*-dimethylamino thiazole **6b** were prepared by 'one-pot' cyclization in refluxing ethanol of *N,N*-dimethylcyanamide with the anion of α -mercapto 3,4,5-trimethoxyacetophenone, generated in situ by treating *O*-ethyl-S-[2-oxo-2-(3,4,5-trimethoxyphenyl)-ethyl] dithiocarbon-

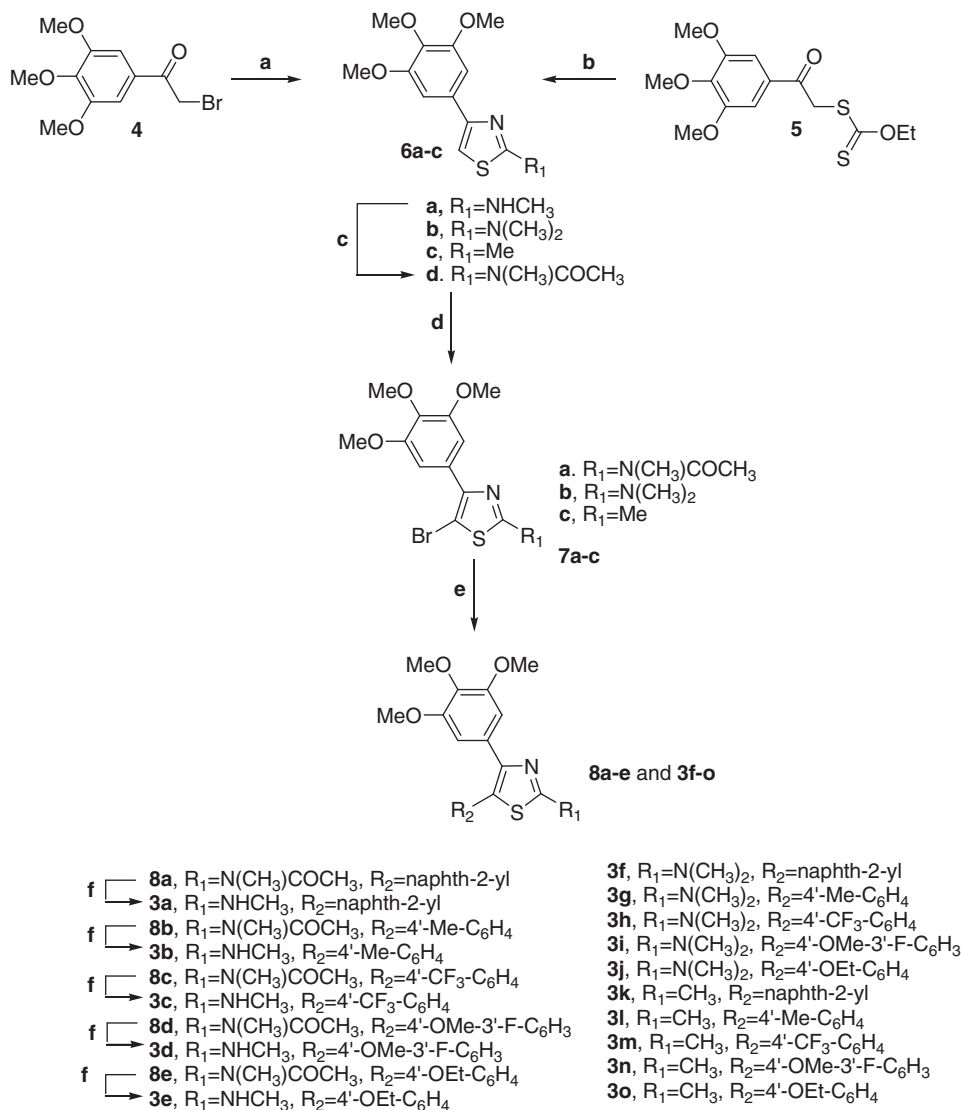
ate **5** with piperidine.¹³ Position 5 of C2-substituted thiazoles **6b–d** was then brominated using *N*-bromosuccinimide in CHCl₃, to yield the 5-bromothiazole derivatives **7a–c**. These molecules were subjected to Suzuki–Miyaura coupling conditions in the presence of various commercially available arylboronic acids, giving rise to the corresponding 5-aryl thiazole derivatives **3f–o** and **8a–e**. These latter compounds were transformed by ethanolysis into the final products **3a–e**.

3. Biological results and discussion

3.1. In vitro antiproliferative activities

The series of 2-substituted-4-(3',4',5'-trimethoxyphenyl)-5-arylthiazoles **3a–o** were evaluated for their inhibition of the growth of a panel of six different human cancer cell lines in comparison with the 2-aminothiazole analogues **2a–e** and the reference compound CA-4 (**1a**) as positive controls. From the antiproliferative data reported in Table 1, the potency of the new synthesized molecules **3a–o** was found to be highly dependent on the substituent at the 2-position of thiazole ring, and, in addition, some interesting trends were noted. The substituent at the 2-position of the thiazole ring clearly affected inhibitory effects on cell growth, with decreasing activity generally observed as follows: NH₂ > NHCH₃ > CH₃ \gg N(CH₃)₂.

With the exception of 4'-trifluoromethylphenyl derivative **3c**, all *N*-methylamino derivatives **3a–e** had significant antiproliferative activity against all tested human cancer cell lines, some of them even had IC₅₀'s in the low to mid nanomolar range. Compound **3e**, bearing 4'-ethoxyphenyl and *N*-methylamino moieties at the 2- and 5-positions, respectively, of thiazole ring displayed the greatest antiproliferative activity among the new synthesized compounds **3a–o**, with IC₅₀ values ranging from 1.7 to 38 nM



Scheme 1. Reagents and conditions: (a) *N*-Methylthiourea or thioacetamide for **6a** and **6c**, respectively, EtOH, reflux; (b) $(\text{CH}_3)_2\text{NCN}$, piperidine, EtOH, reflux; (c) AcONa, Ac₂O, reflux; (d) NBS, CHCl₃, rt for **6b-d**; (e) PdCl₂(DPPF), ArB(OH)₂, CsF, 1,4-dioxane and 65 °C for **7a** and **7c** or toluene and 75 °C for **7b**; (f) 1 N NaOH, EtOH, reflux.

against the six cell lines. Derivative **3e** was 5-, 15- and 1000-fold more potent than CA-4 against A549, MCF-7 and HT-29 cells, but it was 2- to 4-fold less potent than CA-4 against the other three lines. However, compound **3e** was one to two orders of magnitude less active than its 2-aminothiazole counterpart **2e** in four of the six cancer cell lines, the exceptions being the MCF-7 and HT-29 cells, in which **3e** was 2- and 10-fold more potent than **2e**, respectively. In human colon adenocarcinoma HT-29 cells, compound **3e** was 4- to 70-fold more potent than derivatives **2a-e**.

Comparing compounds with the same substituent at the C5-position of the thiazole ring, replacement of the 2-amino group of thiazole derivatives **2a-e** with a *N*-methylamino group (compounds **3a-e**) decreased antiproliferative activity against four of the six cell lines, while with MCF-7 and HT-29 cells there were variable effects. With the exception of 4'-trifluoromethylphenyl derivative **3c**, the MCF-7 breast cancer cell line was more sensitive toward *N*-methylamino analogues **3a-b** and **3d-e** than the corresponding amino counterparts **2a-b** and **2d-e**, with **3b** being the most potent of all the newly synthesized derivatives **3a-o** in this cell line. Moreover, **3b** was almost 28-fold more potent than **2b** against the MCF-7 cells. In HT-29 cells, the 4'-methoxyphenyl

(**3d**) and 4'-ethoxyphenyl (**3e**) derivatives were 2- and 10-fold more potent than their 2-amino counterparts **2d** and **2e**.

Comparing compounds **3k-o**, which shared a common methyl moiety at the thiazole C2-position, the naphth-2-yl derivative **3k** had the highest antiproliferative activities in five of the six human cancer cell lines, the exception being the HT-29 cells, in which **3k** was less active than **3m** and **3o**. All the *N,N*-dimethylamino derivatives **3f-j** showed lower antiproliferative activities than did their *N*-methylamino analogues **3a-e**, and **3f-j** had relatively little activity against all the cell lines examined.

3.2. Effect of compounds **3e** and **3k** on normal human cells

To obtain more insights into the cytotoxic potential of test compounds for normal human cells, the most active compounds were assayed in vitro against peripheral blood lymphocytes (PBL) from healthy donors as previously reported.¹⁴ Compounds **3e** and **3k**, proved moderately cytotoxic having a GI₅₀ of 443 ± 29 and 1272 ± 307 nM in resting PBL, respectively, whereas in PHA-stimulated PBL we found a GI₅₀ of 120 ± 24 (**3e**) and 285 ± 57 nM (**3k**) suggesting that this derivatives acts preferentially on prolifer-

Table 1
In vitro cell growth inhibitory effects of compounds **2a–e**, **3a–o** and CA-4 (**1**)

Compd	IC ₅₀ ^a (nM)					
	HeLa	A549	HL-60	Jurkat	MCF-7	HT-29
2a^b	1.6 ± 0.6	3.8 ± 0.6	2.7 ± 0.3	3.3 ± 0.9	51.2 ± 9.2	23.9 ± 3.9
2b^b	0.73 ± 0.2	42.8 ± 5.7	3.9 ± 1.1	3.9 ± 0.6	279.5 ± 69.8	12.4 ± 5.1
2c^b	3.2 ± 0.4	357 ± 65	5.1 ± 1.1	8.5 ± 1.2	0.4 ± 0.1	221 ± 50.2
2d^b	2.3 ± 0.2	20.2 ± 1.7	3.2 ± 1.2	2.1 ± 0.4	60.9 ± 8.4	11.7 ± 3.9
2e^b	0.03 ± 0.005	0.09 ± 0.01	0.9 ± 0.3	0.14 ± 0.05	44.0 ± 6.3	38.2 ± 11.4
3a	128 ± 49	151 ± 36	143 ± 67	51.1 ± 13	21.1 ± 4.0	38.2 ± 6.1
3b	69.1 ± 13	125 ± 22	18.1 ± 5.2	19.0 ± 8.2	10.1 ± 4.1	423 ± 107
3c	3401 ± 292	4565 ± 536	3166 ± 188	3014 ± 769	7285 ± 851	1235 ± 149
3d	70.1 ± 12.3	138 ± 26	27.3 ± 7.2	34.3 ± 7.2	37.6 ± 14.1	6.3 ± 1.0
3e	13.2 ± 6.3	38.6 ± 7.3	1.8 ± 0.8	1.7 ± 0.8	24.5 ± 14.2	3.2 ± 0.4
3f	1404 ± 222	2900 ± 320	2568 ± 834	836 ± 135	2385 ± 574	729 ± 108
3g	4141 ± 165	3960 ± 465	3479 ± 359	6656 ± 1762	>10,000	3916 ± 1470
3h	>10,000	>10,000	>10,000	>10,000	>10,000	>10,000
3i	3371 ± 366	>10,000	1893 ± 424	7599 ± 1262	8362 ± 1291	497 ± 72
3j	3264 ± 937	>10,000	303 ± 26	4150 ± 1242	>10,000	6027 ± 190
3k	82.1 ± 4.0	119 ± 22	205 ± 37	48.6 ± 11.1	33.4 ± 8.2	702 ± 142
3l	1100 ± 58	1950 ± 156	1512 ± 45	517 ± 192	1743 ± 374	722 ± 235
3m	3826 ± 311	4287 ± 258	>10,000	7109 ± 1677	>10,000	396 ± 164
3n	500 ± 25.2	2563 ± 421	3427 ± 80	1755 ± 838	606 ± 12	1417 ± 250
3o	1866 ± 145	3321 ± 352	253 ± 19	1744 ± 656	42.3 ± 8.2	487 ± 67
CA-4	4 ± 1	180 ± 50	1 ± 0.2	5 ± 0.6	370 ± 100	3100 ± 100

^a IC₅₀ = compound concentration required to inhibit tumor cell proliferation by 50%. Data are expressed as the mean ± SE from the dose–response curves of at least three independent experiments.

^b Data taken from Ref. 12.

ating cells. Nevertheless these results pointed out also that compounds **3e** and **3k** are less cytotoxic respect to the lymphoblastic cell line Jurkat (see Table 1).

3.3. Effect of compounds **3k**, **3d** and **3e** on multidrug resistant cells

To investigate whether these derivatives are substrates of drug efflux pumps, some of the most active compounds (**3d–e**, **3k**) were tested against a panel of drug resistant cell lines that either overexpress P-glycoprotein (Lovo^{Doxo} and Cem^{Vbl100})^{15,16} or are associated with tubulin gene mutations (A549-T12)¹⁷ that result in modified tubulin with impaired polymerization properties. As shown in Table 2, the tested compounds exhibited cytotoxic activ-

Table 2
In vitro cell growth inhibitory effects of compound **3d–e**, **3k** on drug resistant cell lines

Compd	IC ₅₀ ^a (nM)		Resistance ratio ^b
	LoVo	LoVo ^{Doxo}	
3d	190 ± 70	152 ± 14	0.8
3e	31 ± 4.5	14.5 ± 1.2	0.5
3k	72 ± 16	150 ± 25	2.1
Doxorubicin^c	120 ± 30	13150 ± 210	109.6
	CEM	CEM ^{Vbl100}	Resistance ratio ^b
3d	10 ± 3.5	15 ± 4.6	1.5
3e	0.8 ± 0.1	1.2 ± 0.2	2.9
3k	61 ± 18	88 ± 12	1.4
Vinblastine	0.8 ± 0.1	205 ± 46	256.2
	A549	A549-T12	Resistance ratio ^b
3d	138 ± 26	125 ± 23	0.9
3e	38.6 ± 7.3	21.5 ± 9.0	0.5
3k	119 ± 22	121 ± 36	1.0
Taxol^c	7.2 ± 0.1	75.2 ± 12.5	10.4

^a IC₅₀ = compound concentration required to inhibit tumor cell proliferation by 50%. Data are expressed as the mean ± SE from the dose–response curves of at least three independent experiments.

^b The values express the ratio between the IC₅₀'s determined in resistant and non-resistant cell lines.

^c Data from Ref. 8.

ity in all three of the drug resistant cell lines. The activity in the two P-glycoprotein overexpressing cell lines demonstrated that these derivatives are not substrates for this important drug pump.

3.4. Inhibition of tubulin polymerization and colchicine binding

To investigate whether the antiproliferative activities of compounds **3a–b**, **3d–k** and **3o** derived from an interaction with tubulin, these agents were evaluated for their inhibition of tubulin polymerization and for effects on the binding of [³H]colchicine to tubulin.^{18,19} For comparison, 2-amino thiazoles **2a–b** and **2d–e**, as well as CA-4, were examined in contemporaneous experiments. Data for inactive compounds in the assembly assay (IC₅₀ > 20 μM) are not shown in Table 3. All the *N,N*-dimethylamino derivatives **3f–j** did not inhibit tubulin assembly at a concentration as high as 20 μM. Compound **3e** was found to be the most active derivative in the in vitro tubulin polymerization assay (IC₅₀, 0.89 μM). This is in agreement with **3e** being the compound with the greatest antiproliferative activity. Compounds **3a–b**, **3d**, **3k** and **3o** had

Table 3
Inhibition of tubulin polymerization and colchicine binding by compounds **2a–b**, **2d–e**, **3a–b**, **3d–e**, **3k**, **3o** and CA-4

Compd	Tubulin assembly ^a IC ₅₀ (μM)	Colchicine binding ^b (%)
2a	0.74 ± 0.01	94 ± 0.49
2b	0.44 ± 0.01	88 ± 0.71
2d	1.1 ± 0.07	79 ± 0.21
2e	0.61 ± 0.05	95 ± 0.71
3a	0.96 ± 0.01	78 ± 2.1
3b	1.2 ± 0.07	68 ± 1.4
3d	1.3 ± 0.07	61 ± 0.28
3e	0.89 ± 0.06	83 ± 0.28
3k	1.1 ± 0.07	66 ± 0.21
3o	1.2 ± 0.07	51 ± 2.8
CA-4 (1)	1.2 ± 0.07	98 ± 0.42

^a Inhibition of tubulin polymerization. Tubulin was at 10 μM.

^b Inhibition of [³H]colchicine binding. Tubulin, colchicine and tested compound were at 1, 5 and 5 μM, respectively. Data are expressed as the mean ± SE of two independent experiments.

IC₅₀ values of 0.96–1.3 μM, essentially equivalent to that of CA-4 (IC₅₀, 1.2 μM), although **3o** was less effective as an inhibitor of cell growth than CA-4.

When comparing inhibition of tubulin polymerization with antiproliferative effect, we found a good correlation for most of the active compounds, but not for all of them. Thus, compounds **3b**, **3d** and **3o** were similar as inhibitors of tubulin assembly, but **3b** and **3d** were much more active than **3o** as antiproliferative agents.

The free amino group on compounds **2a** and **2e** is not critical for inhibition of tubulin assembly. Substituting the amino group with a methyl, as in compounds **3k** and **3o**, results in retention of activity.

In the colchicine binding studies, derivative **3e** was almost (83% inhibition) as potent as CA-4, which in these experiments inhibited colchicine binding by 98%. Inhibition of colchicine binding by compounds **3b**, **3d**, **3k** and **3o** was lower, varying within the 51–68% range, and they were also less potent than **3a**, which inhibited colchicine binding by 78%. Although, many agents in the present series have activities comparable (**3b**, **3d**, **3k** and **3o**) or superior (**3a** and **3e**) to that of CA-4 as inhibitors of tubulin assembly, none was as active as CA-4 as an inhibitor of colchicine binding to tubulin.

The results are consistent with the conclusion that inhibition of cell growth of these new compounds derives from an interaction with the colchicine site of tubulin and interference with microtubule assembly.

Comparing the antiproliferative activity of 2-*N*-methylamino-thiazole derivatives **3d–e** with those of 2-amino counterparts **2d–e**, the data indicated that a free amino group at the thiazole C2-position was an essential requisite for potent activity. In the inhibition of tubulin assembly, compounds **2d** and **3d**, as well as **2e** and **3e**, exhibited similar antitubulin activity, although both 2-amino derivatives had somewhat greater activity than their methylated analogues. The discrepancy between antiproliferative activity and antitubulin potency has been reported previously. The lower antiproliferative activities of **3d–e** as compared with **2d–e** may result from poor permeability into cells, poor solubility in the tissue culture medium or any other mechanism limiting the accessibility of molecules **3d–e** to cellular tubulin. Nevertheless, we cannot exclude the possibility that **2d–e** may affect other molecular targets in addition to microtubules and thus cause their enhanced antiproliferative activity.

3.5. Molecular modeling

In an attempt to rationalize the biological results observed, a series of molecular docking simulations were carried out following the procedure used previously.¹² Indeed, the binding mode observed for the compounds reported here is very similar to that observed for **2a–e**, with the trimethoxyphenyl ring in close contact with Cys241 and the second aromatic moiety deep in the binding pocket (Fig. 1). Interestingly, the *N,N*-dimethylamino analogues **3f–j** also presented the same binding mode, providing little structural rationale for the loss of biological activity observed with these compounds. More closely examining the docking results (Fig. 2), however, we observed a minor steric clash between the dimethylamino group and tubulin residue Thr179. To assess the significance of this observation, we performed a series of short molecular dynamics (MD) simulations on compounds **2e**, **3e** and **3j** in complex with tubulin. The results obtained clearly show that the presence of the two methyl groups induce a significant conformational change of the binding site residues in close contact with the *N,N*-dimethylamino moiety (Fig. 2). Furthermore, there is a significant shift of the compound itself within the pocket, suggesting an overall binding instability for this compound.

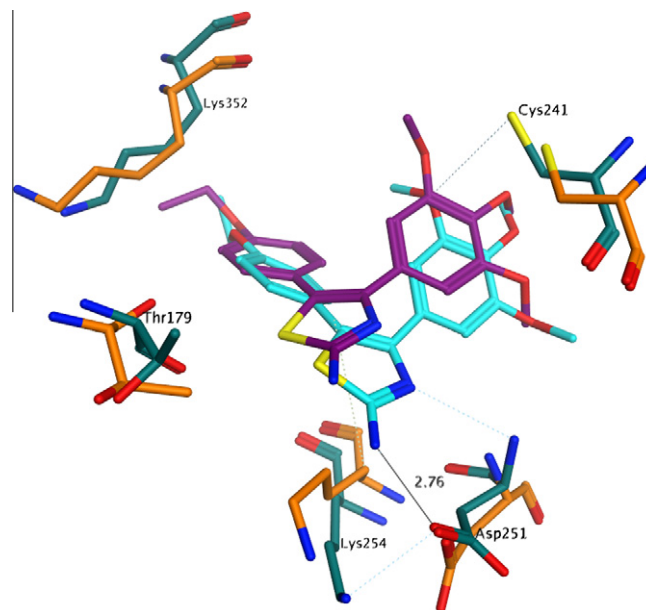


Figure 1. Proposed binding pose of **2e** to tubulin. Before the molecular dynamics: carbon atoms of **2e** in purple, carbon atoms of tubulin residues in orange; after the molecular dynamics: carbon atoms of **2e** in cyan, carbon atoms of tubulin residues in turquoise. Other atoms indicated as follows: red, oxygen; blue, nitrogen; yellow, sulphur; Hydrogen atoms are not shown.

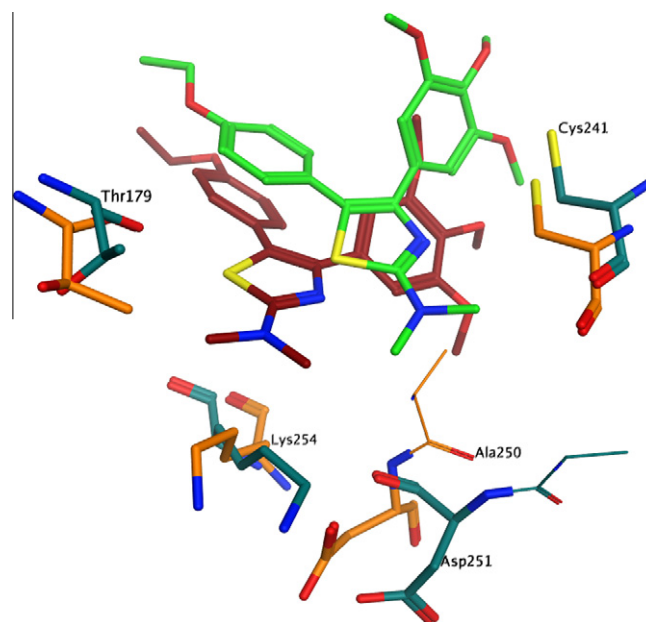


Figure 2. Proposed binding pose of **3j** to tubulin. Before the molecular dynamics: carbon atoms of **3j** in brown, carbon atoms of tubulin residues in orange; after the molecular dynamics: carbon atoms of **3j** in green, carbon atoms of tubulin residues in turquoise. Other atoms indicated as follows: red, oxygen; blue, nitrogen; yellow, sulphur; Hydrogen atoms are not shown.

Moreover, in the case of compound **2e**, the binding complex remained stable during the simulation time, and **2e** also established two hydrogen bonds between the aminothiazole ring and Asp251 (Fig. 1). The simulation on compound **3e** presented a very similar profile to the one observed for **2e** (Fig. 3), confirming the overall binding stability of this compound and providing a possible justification for the different inhibition of tubulin polymerization profiles of **2e**, **3e** and **3j**.

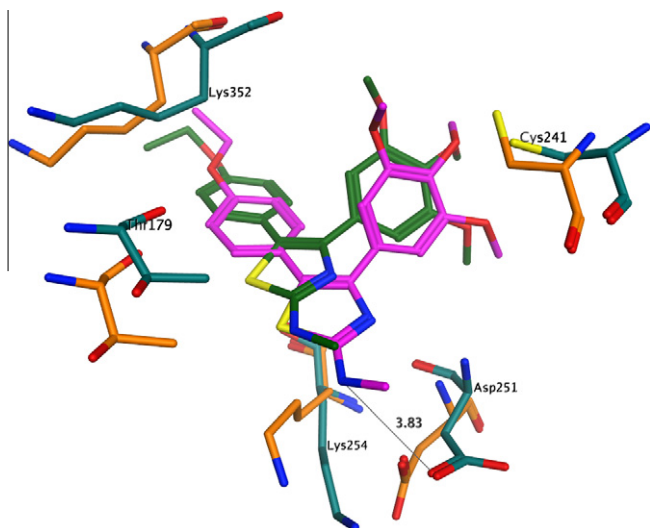


Figure 3. Proposed binding pose of **3e** to tubulin. Before the molecular dynamics: carbon atoms of **3e** in dark green, carbon atoms of tubulin residues in orange; after the molecular dynamics: carbon atoms of **3e** in purple, carbon atoms of tubulin residues in turquoise. Other atoms indicated as follows: red, oxygen; blue, nitrogen; yellow, sulphur; Hydrogen atoms are not shown.

3.6. Analysis of cell cycle effects

The effect of **3e** and **3k** on cell cycle progression was examined by flow cytometry in HeLa and Jurkat cells. **3e** treatment resulted in the rapid accumulation of cells in the G2/M phase, with a concomitant reduction in cells in both the S and G1 phases, in both cell lines. These changes occurred in a concentration-dependent manner (Fig. 4, panels A and B), but changes were observed even at the lowest concentrations (31 nM in HeLa cells, 62 nM in Jurkat cells) used. In contrast, compound **3k** induced an increase in G2/M arrested cells only at higher concentrations (a small rise was first observed with 125 nM compound in both cell lines).

Next, we investigated the association between **3e** and **3k**-induced G2/M arrest and alterations in G2/M regulatory protein expression in HeLa cells. As shown in Figure 4 (panel C), both compounds caused phosphorylation of the phosphatase cdc25c.

The phosphorylation of cdc25c directly stimulates its phosphatase activity, and this is necessary to activate cdc2/cyclin B on entry into mitosis.²⁰ In good agreement, we also observed at both 24 and 48 h of incubation, a dephosphorylation at Tyr15 of cdc2 kinase. The expression of cyclin B remained practically constant after 24 h of treatment with both compounds, followed at 48 h with compound **3e** by a slight decrease in cyclin B expression.

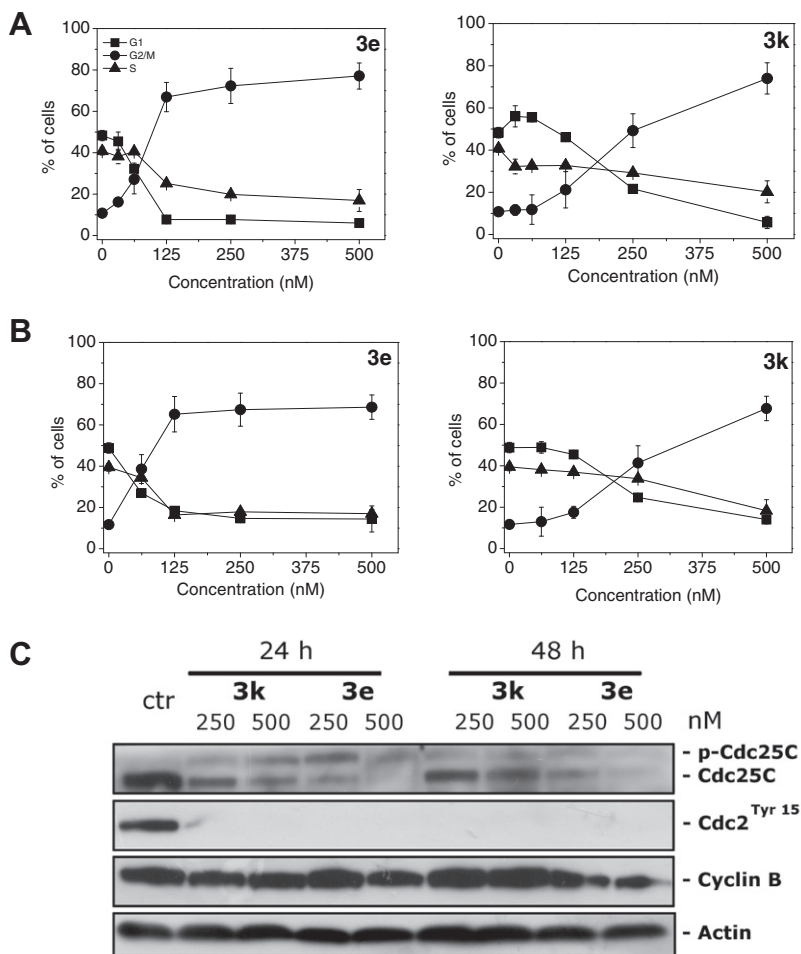


Figure 4. Effect of compounds **3e** and **3k** cell on cycle distribution of HeLa (panel A) and Jurkat cells (panel B). Cells were treated with different compound concentrations ranging from 31 to 500 nM for 24 h. Then the cells were fixed and stained with PI to analyze DNA content by flow cytometry. Data are presented as mean \pm SEM of three independent experiments. Panel C: Effect of **3e** and **3k** on G2/M regulatory proteins. HeLa cells were treated for 24 or 48 h with the indicated concentration of the compound. The cells were harvested and lysed for the detection of cyclin B, p-cdc2^{Y15} and cdc25c expression by western blot analysis. To confirm equal protein loading, each membrane was stripped and reprobed with anti- β -actin antibody.

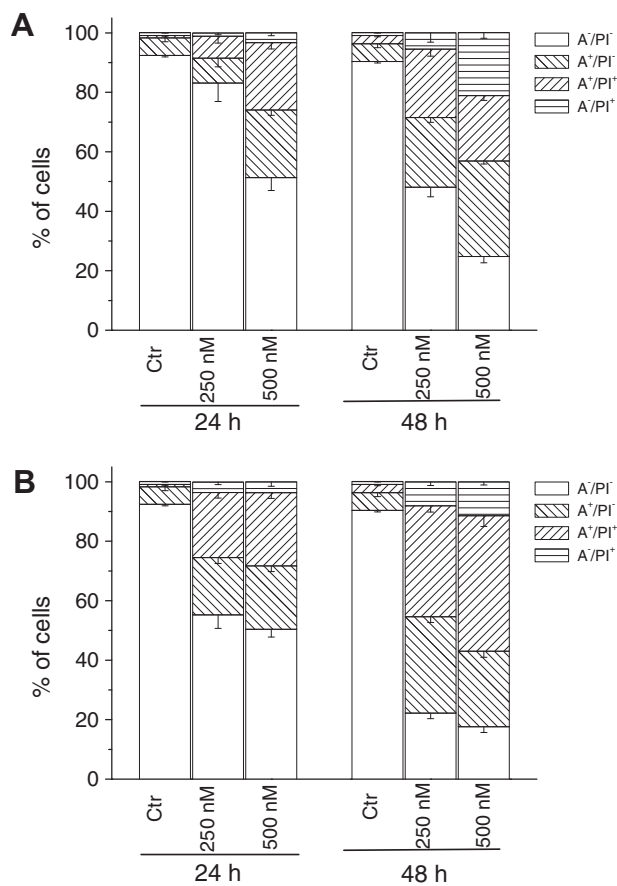


Figure 5. Flow cytometric analysis of apoptotic cells after treatment of HeLa cells with **3k** (panel A) and **3e** (panel B) at the indicated concentrations after incubation for 24 or 48 h. The cells were harvested and labeled with annexin-V-FITC and PI and analyzed by flow cytometry. Data are represented as mean \pm SEM of three independent experiments.

3.7. Compounds **3e** and **3k** induced apoptosis

To evaluate the mode of cell death induced by compounds **3e** and **3k**, we performed a biparametric cytofluorimetric analysis using propidium iodide (PI) and annexin-V-FITC, which stain DNA and phosphatidylserine (PS) residues, respectively.

After treatment with the two compounds at either 250 or 500 nM for 24 or 48 h, HeLa cells were labeled with the two dyes, and the resulting red (PI) and green (FITC) fluorescence was monitored by flow cytometry. As shown in Figure 5 (panel A), **3k** caused a significant induction of apoptotic cells (A⁺/PI⁻ and A⁺/PI⁺) after 24 h, especially with the compound at 500 nM. The percentage of annexin-V positive cells then further increased at 48 h. Analogous behaviour but with a stronger effect was observed for **3e** (Fig. 5, panel B). These data were supported by findings using the MTT assay. These findings prompted us to further investigate the apoptotic process after treatment of cells with **3e** and **3k**.

3.8. Effect of **3e** and **3k** on caspases activation

The activation of caspases plays a central role in apoptotic cell death. To determine which caspases were involved in cell death induced by compounds **3e** and **3k**, the expression of different caspases was measured by immunoblot analysis. We observed a clear activation of caspase-3, as well as cleavage of the caspase-3 substrate PARP, after 24 and 48 h exposures to the two compounds

(Fig. 6, panel A). Of note, treatment with **3e** and **3k** did not induce activation of caspase-9, (data not shown), one of the major initiator caspases in the intrinsic (mitochondrial) apoptosis pathway. In particular, mitochondrial functions such as mitochondrial polarization and ROS production were only slightly affected by treatment with the two compounds (data not shown). Interestingly, we observed a clear caspase-8 and caspase-2 activation following treatment with compounds **3e** and **3k** (Fig. 6, panel A). The activation of caspase-2 is indicated by disappearance of the uncleaved protein in the western blot, while the activation of caspase-8 is indicated by appearance of the cleavage product. In this context, caspase-2 is a unique caspase with characteristics of both initiator and effector caspases.²¹ Recently, its key role in several apoptosis signaling cascades has emerged. In particular, caspase-2 has been implicated in the cell death induced by different antimetabolic agents.^{22,23}

3.9. Effect of **3e** and **3k** on BH3 protein and IAP expression

There is increasing evidence that regulation of the Bcl-2 family of proteins shares the signaling pathways induced by antimicrotubule compounds.^{20a,24} Several pro-apoptotic family proteins (e.g., Bax, Bid, Bim and Bak) promote the release of cytochrome c, whereas anti-apoptotic members (Bcl-2, Mcl-1) are capable of antagonizing the pro-apoptotic proteins and preventing the loss of mitochondrial membrane potential. Our results showed that Bcl-2 expression is strongly reduced after treatment with the two compounds (Fig. 6, panel B), while, in contrast, expression of Bax, a proapoptotic protein of the Bcl-2 family, was unchanged. Mcl-1 is an anti-apoptotic member of the Bcl-2 family, and recently it has been reported that sensitivity to antimetabolic drugs is regulated by Mcl-1 levels.^{25,26} As shown in Figure 6 (panel B) we observed disappearance of the Mcl-1 band after 24 h treatments with both compounds.

Xiap and survivin are members of IAP family (Inhibitors of apoptosis protein), and, in general the IAP proteins function through direct interactions to inhibit the activity of several caspases, including caspase-3, caspase-7 and caspase-9, thereby inhibiting the processing and activation of the caspases.²⁷ Our results (Fig. 6) showed that expression of Xiap was almost eliminated after a 24 h treatment with either compound. Of note, survivin was phosphorylated on Thr32 upon treatment with the two compounds at both 24 and 48 h. This effect is consistent with cell cycle arrest in mitosis.²⁸ In addition, since survivin phosphorylation on Thr32 may regulate apoptosis at cell division via an interaction with caspase-9,²⁹ our results suggest that activation of caspase-2 may be a compensatory mechanism that leads to cell death.

4. Conclusions

In this manuscript we have reported a series of thiazole derivatives modified at their C2-position, which shared with previously published compounds **2a–e**, the 3',4',5'-trimethoxyphenyl and aryl substituents at their C4- and C5-positions, respectively. The results showed that small changes at the 2-position of thiazole ring had a major impact on antiproliferative activity, with the new synthesized compounds **3a–o** generally less active than the corresponding 2-aminothiazole analogues **2a–e**. However, the most potent compound of this series, derivative **3e**, displayed similar or more potent antiproliferative activity than CA-4, with IC₅₀ values ranging from 1.7 to 38 nM against the tested cancer cell lines. Compound **3e** was also the most active inhibitor of tubulin polymerization (IC₅₀ = 0.89 μ M) and strongly inhibited the binding of [³H]colchicine to tubulin (83% inhibition), with activities not greatly different from those of CA-4. For this latter derivative, a good correlation was observed between antiproliferative activity, inhibition of

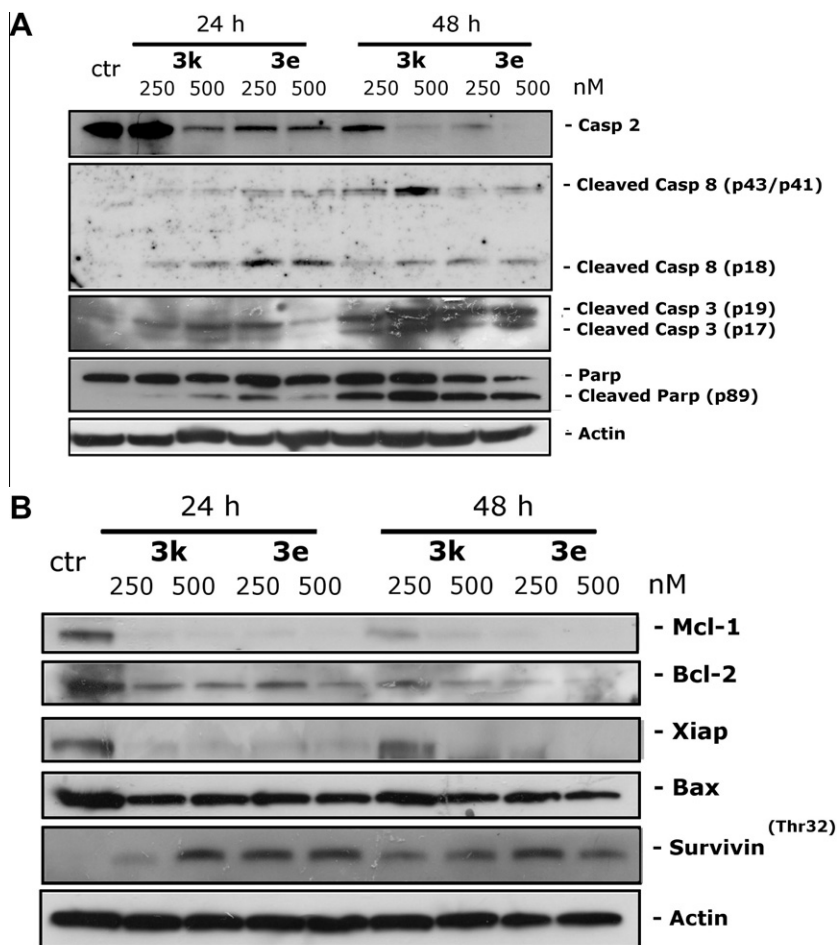


Figure 6. Effect of **3e** and **3k** on the expression of caspases (panel A) and Bcl-2 family members and IAP proteins (panel B). HeLa cells were treated with the indicated concentrations of compounds for 24 or 48 h. Then the cells were harvested and lysed for the detection of protein expression with specific antibodies by western blot analysis.

tubulin polymerization and inhibition of colchicine binding. Comparing compounds characterized by the same substituent at the C5-position of the thiazole ring, with the exception of MCF-7 and HT-29 cells, replacement of the 2-amino group with a *N*-methylamino, *N,N*-dimethylamino and methyl moieties produced a decrease of activity, with the potency decreasing in the following order: $\text{NH}_2 > \text{NHCH}_3 > \text{CH}_3 \gg \text{N}(\text{CH}_3)_2$. With the exception of 4'-trifluorophenyl derivative **2c**, for derivatives **2a–b** and **2d–e** replacement of the amino group with a *N*-methylamino at the 2-position of the thiazole skeleton (compounds **3a–e**) led to an increase in activity against MCF-7 cells. This effect was more evident for the 4'-tolyl analogue **3b**, which was 4- to 30-fold more potent than derivatives **2a–b** and **2d–e**. The reduced antiproliferative activities of compounds **3f–j** indicated that the presence of an additional methyl group on the *N*-methylamino moiety of analogues **3a–e** was detrimental to activity. The 2-*N*-methylamino thiazole derivatives **3d–e** retain the tubulin affinity of the parent 2-amino compounds **2d–e** and CA-4. The greater antiproliferative activity of **2d–e** as compared with **3d–e** despite similar antitubulin effects suggests either differences in intracellular transport or, possibly, an additional cellular target for the former compounds.

The most active compounds strongly induced apoptosis, and this effect was followed by caspase activation. An interesting finding of this study was that, at least in HeLa cells, we did not observe a mitochondrial apoptotic pathway but instead the activation of caspase-8 and caspase-2 following treatment of cells with the most active compounds. In addition, the strong decrease of the anti-apoptotic proteins of Bcl-2 and Mcl-1 along with reduction of Xiap

enhanced the apoptotic pathway induced by this class of compounds.

5. Experimental section

5.1. Chemistry

5.1.1. Materials and methods

^1H NMR spectra were recorded on a Varian VXR 200 spectrometer. Chemical shifts (δ) are given in ppm upfield, and the spectra were recorded in appropriate deuterated solvents, as indicated. Positive-ion electrospray ionization (ESI) mass spectra were recorded on a double-focusing Finnigan MAT 95 instrument with BE geometry. Melting points (mp) were determined on a Buchi-Tottoli apparatus and are uncorrected. All products reported showed ^1H NMR spectra in agreement with the assigned structures. The purity of tested compounds was determined by combustion elemental analyses conducted by the Microanalytical Laboratory of the Chemistry Department of the University of Ferrara with a Yanagimoto MT-5 CHN recorder elemental analyzer. All tested compounds yielded data consistent with a purity of at least 95% as compared with the theoretical values. All reactions were carried out under an inert atmosphere of dry nitrogen, unless otherwise indicated. Standard syringe techniques were used for transferring dry solvents. Reaction courses and product mixtures were routinely monitored by TLC on silica gel (precoated F_{254} Merck plates), and compounds were visualized with aqueous KMnO_4 . Flash chromatography was performed using 230–400

mesh silica gel and the indicated solvent system. Organic solutions were dried over anhydrous Na₂SO₄. Arylboronic acids are commercially available and used as received. All chemicals and reagents were purchased from Aldrich (Sigma–Aldrich) or Lancaster (Alfa Aesar, Johnson Matthey Company).

5.2. General procedure (A) for the synthesis of compounds (6a) and (6c)

A mixture of 2-bromo-1-(3,4,5-trimethoxyphenyl)ethanone **4** (1.45 g, 5 mmol) and thioacetamide or *N*-methylthiourea (5.5 mmol) in anhydrous EtOH (20 mL) was heated to reflux for 1.5 h. After that, the solvent was removed in vacuo, and saturated aqueous NaHCO₃ (5 mL) was added to make the mixture basic (pH 8–9). Then the mixture was extracted with CH₂Cl₂ (3 × 15 mL). The combined organic phases were washed with water (10 mL) and brine (10 mL), dried with anhydrous Na₂SO₄ and concentrated under vacuum.

5.2.1. Synthesis of 4-(3,4,5-trimethoxyphenyl)-*N*-methylthiazol-2-amine (6a)

Following general procedure (A), after work-up the orange oil residue was suspended in ethyl ether (20 mL) and stirred for 1 h at +4 °C. The solid was collected by filtration to give the title compound **6a** as a white powder. Yield 56%, mp 123–125 °C. ¹H NMR (CDCl₃) δ: 2.99 (d, *J* = 5.2 Hz, 3H), 3.88 (s, 3H), 3.92 (s, 6H), 5.34 (bs, 1H), 6.64 (s, 1H), 7.03 (s, 2H). MS (ESI): [M]⁺ = 280.4.

5.2.2. Synthesis of 4-(3,4,5-trimethoxyphenyl)-2-methylthiazole (6c)

Following general procedure (A), after work-up the title compound **6c** was obtained as an oil, which became a white solid at +4 °C. Yield 96%, mp 82–83 °C. ¹H NMR (CDCl₃) δ: 2.77 (s, 3H), 3.87 (s, 3H), 3.92 (s, 6H), 7.11 (s, 2H), 7.23 (s, 1H). MS (ESI): [M]⁺ = 265.5.

5.3. Synthesis of 4-(3,4,5-trimethoxyphenyl)-*N,N*-dimethylthiazol-2-amine (6b)

Piperidine (0.88 mL, 8.8 mmol) was added to a stirred solution of dithiocarbonic acid *O*-ethyl ester *S*-[2-oxo-2-(3,4,5-trimethoxyphenyl)-ethyl] ester **5** (1.32 g, 4 mmol) dissolved in ethanol (20 mL). The reaction mixture was stirred for 30 min at room temperature, and *N,N*-dimethylcyanamide (0.32 mL, 4 mmol) was added. The solution was stirred at reflux for 4 h, after which ethanol was removed under reduced pressure and the residue portioned in a mixture of dichloromethane (15 mL) and a 3 N aqueous solution of HCl (30 mL). The aqueous acid phase was basified (pH 9) with sodium carbonate and washed with dichloromethane (3 × 15 mL). The combined organic phase was washed with brine (10 mL) and dried over sodium sulfate. After concentration under reduced pressure, the residue was triturated with petroleum ether (10 mL), and this furnished the final compound as a brown solid. Yield: 62%, mp 80–81 °C. ¹H NMR (CDCl₃) δ: 3.15 (s, 6H), 3.86 (s, 3H), 3.92 (s, 6H), 6.62 (s, 1H), 7.07 (s, 2H). MS (ESI): [M]⁺ = 294.4.

5.4. Synthesis of *N*-(4-(3,4,5-trimethoxyphenyl)thiazol-2-yl)-*N*-methylacetamide (6d)

Sodium acetate (250 mg, 3 mmol) was added to a stirred solution of **6a** (840 mg, 3 mmol) in acetic anhydride (30 mL). The mixture was refluxed for 18 h, the solvent evaporated in vacuo and the residue portioned in a mixture of dichloromethane (25 mL) and water (10 mL). The organic extract was washed with brine (10 mL), dried over Na₂SO₄ and concentrated at reduced pressure.

The crude product suspended in petroleum ether (15 mL) and stirred for 1 h, furnished the title compound **6d** as a brownish solid. Yield: 89%, mp 197–198 °C. ¹H NMR (CDCl₃) δ: 2.44 (s, 3H), 3.82 (s, 3H), 3.88 (s, 3H), 3.94 (s, 6H), 7.10 (s, 1H), 7.12 (s, 2H). MS (ESI): [M]⁺ = 322.5.

5.5. General procedure (B) for the synthesis of compounds (7a–c)

A solution of the appropriate thiazole **6b–d** (2 mmol) in anhydrous chloroform (10 mL) was cooled to 0 °C and treated with *N*-bromosuccinimide (392 mg, 2.2 mmol) under nitrogen. The reaction was allowed to warm to room temperature and then stirred for 4 h. After quenching with saturated Na₂S₂O₃ (5 mL), the resulting mixture was diluted with dichloromethane (10 mL). The organic phase was washed with water (5 mL) and brine (5 mL), dried (MgSO₄) and evaporated.

5.5.1. Synthesis of *N*-(5-bromo-4-(3,4,5-trimethoxyphenyl)thiazol-2-yl)-*N*-methylacetamide (7a)

Following general procedure (B), after work-up the solid residue was stirred in ethyl ether (10 mL) for 30 min. After filtration, the title compound **7a** was isolated as a cream coloured solid. Yield 86%, mp 177–178 °C. ¹H NMR (CDCl₃) δ: 2.43 (s, 3H), 3.74 (s, 3H), 3.86 (s, 3H), 3.92 (s, 6H), 7.22 (s, 2H). MS (ESI): [M]⁺ = 400.3, [M+2]⁺ = 402.5.

5.5.2. Synthesis of 5-bromo-4-(3,4,5-trimethoxyphenyl)-*N,N*-dimethylthiazol-2-amine (7b)

Following general procedure (B), after work-up the residue was purified by column chromatography, using ethyl acetate/petroleum ether 6–4 v/v as eluent, to afford **7b** as a white solid. Yield 68%, mp 96–97 °C. ¹H NMR (CDCl₃) δ: 3.10 (s, 3H), 3.11 (s, 3H), 3.87 (s, 3H), 3.91 (s, 6H), 7.16 (s, 2H). MS (ESI): [M]⁺ = 372.2, [M+2]⁺ = 374.3.

5.5.3. Synthesis of 5-bromo-4-(3,4,5-trimethoxyphenyl)-2-methylthiazole (7c)

Following general procedure (B), after work-up the residue was purified by column chromatography, using ethyl acetate/petroleum ether 3–7 v/v as eluent, to afford a colorless oil, which, when triturated with hexane, furnished **7c** as a white solid. Yield 74%, mp 98–99 °C. ¹H NMR (CDCl₃) δ: 2.70 (s, 3H), 3.89 (s, 3H), 3.93 (s, 6H), 7.15 (s, 2H). MS (ESI): [M]⁺ = 343.1, [M+2]⁺ = 345.1.

5.6. General procedure (C) for the synthesis of compounds 3k–o and 8a–e

A stirred suspension of 5-bromo-4-(3,4,5-trimethoxyphenyl)-thiazole derivative **7a** or **7c** (0.5 mmol) and the appropriate phenylboronic acid (1 mmol) in dioxane (6 mL containing 3 drops of water) was degassed under a stream of nitrogen for 10 min, then treated with [1,1'-bis(diphenylphosphino)ferrocene] dichloropalladium(II) methylene chloride complex (41 mg, 0.05 mmol) and cesium fluoride (190 mg, 1.25 mmol). The reaction mixture was heated under nitrogen at 45 °C for 30 min, then at 65 °C for 5 h. The reaction mixture was cooled to ambient temperature, diluted with CH₂Cl₂ (10 mL), filtered through a pad of celite and evaporated in vacuo. The residue was dissolved with CH₂Cl₂ (15 mL), and the resultant solution was washed sequentially with water (5 mL) and brine (5 mL). The organic layer was dried and evaporated, and the residue was purified by flash chromatography on silica gel.

5.6.1. 4-(3,4,5-Trimethoxyphenyl)-2-methyl-5-(naphthalen-2-yl)thiazole (3k)

Following general procedure (C), the crude residue, purified by flash chromatography using ethyl acetate/petroleum ether 6:4

(v:v) as eluent furnished **3k** as a yellow oil. Yield 71%. ¹H NMR (CDCl₃) δ: 2.78 (s, 3H), 3.58 (s, 6H), 3.82 (s, 3H), 6.77 (s, 2H), 7.34 (d, *J* = 8.8 Hz, 1H), 7.44 (m, 2H), 7.79 (m, 3H), 7.88 (s, 1H). MS (ESI): [M]⁺ = 391.3. Anal. (C₂₃H₂₁NO₃S): C, H, N.

5.6.2. 4-(3,4,5-Trimethoxyphenyl)-2-methyl-5-*p*-tolylthiazole (3l)

Following general procedure (C), the crude residue, purified by flash chromatography using ethyl acetate/petroleum ether 4:6 (v:v) as eluent, furnished **3l** as a yellow oil. Yield 71%. ¹H NMR (CDCl₃) δ: 2.34 (s, 3H), 2.77 (s, 3H), 3.66 (s, 6H), 3.72 (s, 3H), 6.70 (s, 2H), 7.10 (d, *J* = 8.2 Hz, 2H), 7.23 (d, *J* = 8.2 Hz, 2H). MS (ESI): [M]⁺ = 355.5. Anal. (C₂₀H₂₁NO₃S): C, H, N.

5.6.3. 5-(4-(Trifluoromethyl)phenyl)-4-(3,4,5-trimethoxyphenyl)-2-methylthiazole (3m)

Following general procedure (C), the crude residue, purified by flash chromatography using ethyl acetate/petroleum ether 4:6 (v:v) as eluent, furnished **3m** as a colorless oil. Yield 66%. ¹H NMR (CDCl₃) δ: 2.77 (s, 3H), 3.66 (s, 6H), 3.84 (s, 3H), 6.67 (s, 2H), 7.49 (d, *J* = 8.4 Hz, 2H), 7.57 (d, *J* = 8.8 Hz, 2H). MS (ESI): [M]⁺ = 409.2. Anal. (C₂₀H₁₈F₃NO₃S): C, H, N.

5.6.4. 4-(3,4,5-Trimethoxyphenyl)-5-(4-methoxyphenyl)-2-methylthiazole (3n)

Following general procedure (C), the crude residue, purified by flash chromatography using ethyl acetate/petroleum ether 6:4 (v:v) as eluent, furnished **3n** as a colorless oil. Yield 68%. ¹H NMR (CDCl₃) δ: 2.73 (s, 3H), 3.68 (s, 6H), 3.81 (s, 3H), 3.83 (s, 3H), 6.74 (s, 2H), 6.86 (d, *J* = 8.8 Hz, 2H), 7.26 (d, *J* = 8.8 Hz, 2H). MS (ESI): [M]⁺ = 371.3. Anal. (C₂₀H₂₁NO₄S): C, H, N.

5.6.5. 5-(4-Ethoxyphenyl)-4-(3,4,5-trimethoxyphenyl)-2-methylthiazole (3o)

Following general procedure (C), the crude residue, purified by flash chromatography using ethyl acetate/petroleum ether 4:6 (v:v) as eluent, furnished **3o** as a yellow oil. Yield 79%. ¹H NMR (CDCl₃) δ: 1.41 (t, *J* = 6.8 Hz, 3H), 2.73 (s, 3H), 3.68 (s, 6H), 3.83 (s, 3H), 4.04 (q, *J* = 6.8 Hz, 2H), 6.75 (s, 2H), 6.84 (d, *J* = 8.8 Hz, 2H), 7.26 (d, *J* = 8.8 Hz, 2H). MS (ESI): [M]⁺ = 385.5. Anal. (C₂₁H₂₃NO₄S): C, H, N.

5.6.6. *N*-(4-(3,4,5-Trimethoxyphenyl)-5-(naphthalen-2-yl)thiazol-2-yl)-*N*-methylacetamide (8a)

Following general procedure (C), the crude residue, purified by flash chromatography using ethyl acetate/petroleum ether 4:6 (v:v) as eluent, furnished the **8a** precursor as a colorless oil. Yield 82%. ¹H NMR (CDCl₃) δ: 2.46 (s, 3H), 3.58 (s, 6H), 3.70 (s, 3H), 3.81 (s, 3H), 6.82 (s, 2H), 7.46 (m, 3H), 7.78 (m, 3H), 7.93 (s, 1H). MS (ESI): [M]⁺ = 448.5.

5.6.7. *N*-(4-(3,4,5-Trimethoxyphenyl)-5-*p*-tolylthiazol-2-yl)-*N*-methylacetamide (8b)

Following general procedure (C), the crude residue, purified by flash chromatography using ethyl acetate/petroleum ether 4:6 (v:v) as eluent, furnished **8b** as a yellow oil. Yield 71%. ¹H NMR (CDCl₃) δ: 2.34 (s, 3H), 2.44 (s, 3H), 3.67 (s, 6H), 3.78 (s, 3H), 3.84 (s, 3H), 6.78 (s, 2H), 7.16 (d, *J* = 8.2 Hz, 2H), 7.28 (d, *J* = 8.2 Hz, 2H). MS (ESI): [M]⁺ = 412.5.

5.6.8. *N*-(5-(4-(Trifluoromethyl)phenyl)-4-(3,4,5-trimethoxyphenyl)thiazol-2-yl)-*N*-methylacetamide (8c)

Following general procedure (C), the crude residue, purified by flash chromatography using ethyl acetate/petroleum ether 4:6 (v:v) as eluent, furnished **8c** as a colorless oil. Yield 67%. ¹H NMR

(CDCl₃) δ: 2.46 (s, 3H), 3.70 (s, 6H), 3.75 (s, 3H), 3.84 (s, 3H), 6.71 (s, 2H), 7.49 (d, *J* = 8.4 Hz, 2H), 7.58 (d, *J* = 8.4 Hz, 2H). MS (ESI): [M]⁺ = 466.5.

5.6.9. *N*-(4-(3,4,5-Trimethoxyphenyl)-5-(4-methoxyphenyl)thiazol-2-yl)-*N*-methylacetamide (8d)

Following general procedure (C), the crude residue, purified by flash chromatography using ethyl acetate/petroleum ether 4:6 (v:v) as eluent, furnished **8d** as a yellow oil. Yield: 69% yield. ¹H NMR (CDCl₃) δ: 2.44 (s, 3H), 3.68 (s, 6H), 3.78 (s, 3H), 3.81 (s, 3H); 3.84 (s, 3H), 6.80 (s, 2H), 6.87 (d, *J* = 8.8 Hz, 2H), 7.31 (d, *J* = 8.8 Hz, 2H). MS (ESI): [M]⁺ = 428.6.

5.6.10. *N*-(5-(4-Ethoxyphenyl)-4-(3,4,5-trimethoxyphenyl)thiazol-2-yl)-*N*-methylacetamide (8e)

Following general procedure (C), the crude residue, purified by flash chromatography using ethyl acetate/petroleum ether 4:6 (v:v) as eluent, furnished **8e** as a colorless oil. Yield 72%. ¹H NMR (CDCl₃) δ: 1.41 (t, *J* = 6.8 Hz, 3H), 2.44 (s, 3H), 3.68 (s, 6H), 3.78 (s, 3H), 3.83 (s, 3H); 4.05 (q, *J* = 6.8 Hz, 2H), 6.81 (s, 2H), 6.86 (d, *J* = 8.6 Hz, 2H), 7.29 (d, *J* = 8.6 Hz, 2H). MS (ESI): [M]⁺ = 442.5.

5.7. General procedure (D) for the synthesis of compounds (3a–e)

A mixture of *N*-acetyl thiazole derivative **8a–e** (0.5 mmol), 1 N aqueous NaOH (0.55 mL, 0.55 mmol) and EtOH (8 mL) was refluxed for 1 h, and the solvent was removed by evaporation. The residue was dissolved in a mixture of water (5 mL) and dichloromethane (10 mL). The organic phase was washed with brine (5 mL), dried (Na₂SO₄) and concentrated in vacuo. Ethyl ether (5 mL) was added to the residue, and the resulting precipitate was collected by filtration to furnish the title compound as a solid.

5.7.1. 4-(3,4,5-Trimethoxyphenyl)-*N*-methyl-5-(naphthalen-2-yl)thiazol-2-amine (3a)

Following general procedure (D), after work-up **3a** was isolated as a white solid. Yield 81%, mp 194–195 °C. ¹H NMR (CDCl₃) δ: 3.03 (d, *J* = 4.8 Hz, 3H), 3.59 (s, 6H), 3.83 (s, 3H), 5.25 (bs, 1H), 6.76 (s, 2H), 7.34 (d, *J* = 6.8 Hz, 1H), 7.47 (m, 2H), 7.72 (m, 3H), 7.84 (s, 1H). MS (ESI): [M]⁺ = 406.7. Anal. (C₂₃H₂₂N₂O₃S): C, H, N.

5.7.2. 4-(3,4,5-Trimethoxyphenyl)-*N*-methyl-5-*p*-tolylthiazol-2-amine (3b)

Following general procedure (D), after work-up **3b** was isolated as a yellow solid. Yield 82%, mp 189–190 °C. ¹H NMR (CDCl₃) δ: 2.32 (s, 3H), 2.98 (d, *J* = 5.2 Hz, 3H), 3.67 (s, 6H), 3.82 (s, 3H), 5.22 (bs, 1H), 6.72 (s, 2H), 7.09 (d, *J* = 8.0 Hz, 2H), 7.20 (d, *J* = 8.0 Hz, 2H). MS (ESI): [M]⁺ = 370.5. Anal. (C₂₀H₂₂N₂O₃S): C, H, N.

5.7.3. 5-(4-(Trifluoromethyl)phenyl)-4-(3,4,5-trimethoxyphenyl)-*N*-methylthiazol-2-amine (3c)

Following general procedure (D), after work-up **3c** was isolated as a white solid. Yield 78%, mp 183–184 °C. ¹H NMR (CDCl₃) δ: 4.03 (d, *J* = 5.2 Hz, 3H), 3.67 (s, 6H), 3.84 (s, 3H), 5.23 (bs, 1H), 6.69 (s, 2H), 7.37 (d, *J* = 8.8 Hz, 2H), 7.52 (d, *J* = 8.8 Hz, 2H). MS (ESI): [M]⁺ = 424.9. Anal. (C₂₀H₁₉F₃N₂O₃S): C, H, N.

5.7.4. 4-(3,4,5-Trimethoxyphenyl)-5-(4-methoxyphenyl)-*N*-methylthiazol-2-amine (3d)

Following general procedure (D), after work-up **3d** was isolated as a brown solid. Yield 84%, mp 174–176 °C. ¹H NMR (CDCl₃) δ: 2.99 (d, *J* = 4.4 Hz, 3H), 3.67 (s, 6H), 3.79 (s, 3H), 3.82 (s, 3H), 5.20 (bs, 1H), 6.73 (s, 2H), 6.83 (d, *J* = 8.8 Hz, 2H), 7.23 (d, *J* = 8.8 Hz, 2H). MS (ESI): [M]⁺ = 386.6. Anal. (C₂₀H₂₂N₂O₄S): C, H, N.

5.7.5. 5-(4-Ethoxyphenyl)-4-(3,4,5-trimethoxyphenyl)-*N*-methylthiazol-2-amine (3e)

Following general procedure (D), after work-up **3e** was isolated as a white solid. Yield 82%, mp 136–137 °C. ¹H NMR (CDCl₃) δ: 1.40 (t, *J* = 7.0 Hz, 3H), 2.99 (d, *J* = 5.2 Hz, 3H), 3.67 (s, 6H), 3.82 (s, 3H), 4.03 (q, *J* = 7.0 Hz, 2H), 5.20 (bs, 1H), 6.73 (s, 2H), 6.82 (d, *J* = 8.8 Hz, 2H), 7.21 (d, *J* = 8.8 Hz, 2H). MS (ESI): [M]⁺ = 400.7. Anal. (C₂₁H₂₄N₂O₄S): C, H, N.

5.8. General procedure (E) for the synthesis of compounds 3f–j

To a stirred suspension of **7b** (0.5 mmol) and the appropriate phenylboronic acid (1 mmol) in toluene (7 mL) was added [1,1'-bis(diphenylphosphino)ferrocene]dichloropalladium (II) methylene chloride complex (41 mg, 0.05 mmol) and cesium fluoride (190 mg, 1.25 mmol). The reaction mixture was heated under nitrogen at 55 °C for 45 min, then at 75 °C for 20 h. The reaction mixture was cooled to ambient temperature, diluted with CH₂Cl₂ (10 mL), filtered through a pad of celite and evaporated in vacuo. The residue was dissolved with CH₂Cl₂ (15 mL), and the resultant solution was washed sequentially with water (5 mL) and brine (5 mL). The organic layer was dried and evaporated, and the residue was purified by flash chromatography on silica gel.

5.8.1. 4-(3,4,5-Trimethoxyphenyl)-*N,N*-dimethyl-5-(naphthalen-3-yl)thiazol-2-amine (3f)

Following general procedure E, the crude residue, purified by flash chromatography using ethyl acetate/petroleum ether 2.5:7.5 (v:v) as eluent, furnished **3f** as a yellow oil. Yield 63%. ¹H NMR (CDCl₃) δ: 3.18 (s, 6H), 3.58 (s, 6H), 3.82 (s, 3H), 6.80 (s, 2H), 7.34 (d, *J* = 8.8 Hz, 1H), 7.42 (m, 2H), 7.76 (m, 3H), 7.88 (s, 1H). MS (ESI): [M]⁺ = 420.6. Anal. (C₂₄H₂₄N₂O₃S): C, H, N.

5.8.2. 4-(3,4,5-Trimethoxyphenyl)-*N,N*-dimethyl-5-*p*-tolylthiazol-2-amine (3g)

Following general procedure (E), the crude residue, purified by flash chromatography using ethyl acetate/petroleum ether 3:7 (v:v) as eluent, furnished **3g** as a brown solid. Yield 67%, mp 77–78 °C. ¹H NMR (CDCl₃) δ: 2.32 (s, 3H), 3.14 (s, 3H), 3.15 (s, 3H), 3.66 (s, 6H), 3.82 (s, 3H), 6.76 (s, 2H), 7.10 (d, *J* = 8.0 Hz, 2H), 7.18 (d, *J* = 8.0 Hz, 2H). MS (ESI): [M]⁺ = 384.5. Anal. (C₂₁H₂₄N₂O₃S): C, H, N.

5.8.3. 5-(4-(Trifluoromethyl)phenyl)-4-(3,4,5-trimethoxyphenyl)-*N,N*-dimethylthiazol-2-amine (3h)

Following general procedure (E), the crude residue, purified by flash chromatography using ethyl acetate/petroleum ether 4:6 (v:v) as eluent, furnished **3h** as an orange oil. Yield 68%. ¹H NMR (CDCl₃) δ: 3.17 (s, 6H), 3.68 (s, 6H), 3.83 (s, 3H), 6.69 (s, 2H), 7.37 (d, *J* = 8.2 Hz, 2H), 7.50 (d, *J* = 8.2 Hz, 2H). MS (ESI): [M]⁺ = 438.6. Anal. (C₂₁H₂₁F₃N₂O₃S): C, H, N.

5.8.4. 4-(3,4,5-Trimethoxyphenyl)-5-(4-methoxyphenyl)-*N,N*-dimethylthiazol-2-amine (3i)

Following general procedure (E), the crude residue, purified by flash chromatography using ethyl acetate/petroleum ether 3:7 (v:v) as eluent, furnished **3i** as a cream colored solid. Yield 72%, mp 140–142 °C. ¹H NMR (CDCl₃) δ: 3.14 (s, 6H), 3.67 (s, 6H), 3.79 (s, 3H), 3.81 (s, 3H), 6.76 (s, 2H), 6.82 (d, *J* = 8.8 Hz, 2H), 7.22 (d, *J* = 8.8 Hz, 2H). MS (ESI): [M]⁺ = 400.6. Anal. (C₂₁H₂₄N₂O₄S): C, H, N.

5.8.5. 5-(4-Ethoxyphenyl)-4-(3,4,5-trimethoxyphenyl)-*N,N*-dimethylthiazol-2-amine (3j)

Following general procedure (E), the crude residue, purified by flash chromatography using ethyl acetate/petroleum ether 2.5:7.5 (v:v) as eluent, furnished **3j** as a red oil. Yield 73%. ¹H NMR (CDCl₃)

δ: 1.38 (t, *J* = 7.0 Hz, 3H), 3.14 (s, 6H), 3.67 (s, 6H), 3.81 (s, 3H), 4.02 (q, *J* = 7.0 Hz, 2H), 6.77 (s, 2H), 6.81 (d, *J* = 8.8 Hz, 2H), 7.22 (d, *J* = 8.8 Hz, 2H). MS (ESI): [M]⁺ = 414.6. Anal. (C₂₂H₂₆N₂O₄S): C, H, N.

5.9. Biology experiments

5.9.1. Antiproliferative assays

Human T-leukemia (Jurkat) and human promyelocytic leukemia (HL-60) cells were grown in RPMI-1640 medium, (Gibco, Milano, Italy). Breast adenocarcinoma (MCF-7), human non-small cell lung carcinoma (A549), human cervix carcinoma (HeLa) and human colon adenocarcinoma (HT-29) cells were grown in DMEM medium (Gibco, Milano, Italy). Both media were supplemented with 115 units/mL of penicillin G (Gibco, Milano, Italy), 115 µg/mL of streptomycin (Invitrogen, Milano, Italy) and 10% fetal bovine serum (Invitrogen, Milano, Italy). All these cell lines were purchased by ATCC. LoVo^{Doxo} cells are a doxorubicin resistant subclone of LoVo cells¹⁵ and were grown in complete Ham's F12 medium supplemented with doxorubicin (0.1 µg/mL). CEM^{Vbl-100} cells are a multidrug-resistant line selected against vinblastine.¹⁶ LoVo^{Doxo} and CEM^{Vbl-100} were a kind gift of Dr. G. Arancia (Istituto Superiore di Sanità, Rome, Italy) A549-T12 cells are a non-small cell lung carcinoma line exhibiting resistance to taxol¹⁷ were kindly donated by Professor I. Castagliuolo (University of Padova). They were grown in complete DMEM medium supplemented with taxol (12 nM). Stock solutions (10 mM) of the different compounds were obtained by dissolving them in DMSO. Individual wells of a 96-well tissue culture microtiter plate were inoculated with 100 µL of complete medium containing 8 × 10³ cells. The plates were incubated at 37 °C in a humidified 5% CO₂ incubator for 18 h prior to the experiments. After medium removal, 100 µL of fresh medium containing the test compound at different concentrations was added to each well and incubated at 37 °C for 72 h. The percentage of DMSO in the medium never exceeded 0.25%. This was also the maximum DMSO concentration in all cell-based assays described below. Cell viability was assayed by the (3-(4,5-dimethylthiazol-2-yl)-2,5-diphenyl tetrazolium bromide test as previously described.³⁰ The IC₅₀ was defined as the compound concentration required to inhibit cell proliferation by 50%, in comparison with cells treated with the maximum amount of DMSO (0.25%) and considered as 100% viability.

5.9.2. Effects on tubulin polymerization and on colchicine binding to tubulin

To evaluate the effect of the compounds on tubulin assembly in vitro,¹⁸ varying concentrations of compounds were preincubated with 10 µM bovine brain tubulin in glutamate buffer at 30 °C for 15 min and then cooled to 0 °C. After addition of 0.4 mM GTP, the mixtures were transferred to 0 °C cuvettes in a recording spectrophotometer and warmed to 30 °C. Tubulin assembly was followed turbidimetrically at 350 nm. The IC₅₀ was defined as the compound concentration that inhibited the extent of assembly by 50% after a 20 min incubation. The capacity of the test compounds to inhibit colchicine binding to tubulin was measured as described,¹⁹ except that the reaction mixtures contained 1 µM tubulin, 5 µM [³H]colchicine and 5 µM test compound.

5.9.3. Molecular modeling

All molecular modeling studies were performed on a MacPro dual 2.66 GHz Xeon running Ubuntu 10. The tubulin structure was downloaded from the PDB data bank (<http://www.rcsb.org/>—PDB code:1SAO).³¹ Hydrogen atoms were added to the protein, using the Protonate3D function of molecular operating environment (MOE).³² Ligand structures were built with MOE and minimized using the MMFF94x forcefield until a RMSD gradient of 0.05 kcal mol⁻¹ Å⁻¹ was reached. The docking simulations were

performed using plants.³³ Molecular dynamics was performed with the Gromacs 4.5³⁴ with the Amber99 force field. The structure was solvated using TIP3P water molecules, providing a minimum of 9.0 Å of water between the protein surface and any periodic box edge. The system was neutralized, minimized and then a position restrain dynamics simulation was carried out for 150 ps. The production simulation was conducted for 2 ns at 298 K using a NPT environment. Inhibitors were parameterized by Antechamber of AmberTool 1.5.³⁵ Trajectories analysis were carried out by VMD.³⁵

5.9.4. Flow cytometric analysis of cell cycle distribution

For flow cytometric analysis of DNA content, 5×10^5 HeLa or Jurkat cells in exponential growth were treated with different concentrations of the test compounds for 24 or 48 h. After incubation, the cells were collected, centrifuged and fixed with ice-cold ethanol (70%). The cells were treated with lysis buffer containing RNase A and 0.1% Triton X-100 and stained with PI. Samples were analyzed on a Cytomic FC500 flow cytometer (Beckman Coulter). DNA histograms were analyzed using MultiCycle[®] for Windows (Phoenix Flow Systems).

5.9.5. Annexin-V assay

Surface exposure of PS on apoptotic cells was measured by flow cytometry with a Coulter Cytomics FC500 (Beckman Coulter) by adding annexin-V-FITC to cells according to the manufacturer's instructions (Annexin-V Fluos, Roche Diagnostic). Simultaneously, the cells were stained with PI.

5.9.6. Western blot analysis

HeLa cells were incubated in the presence of test compounds and, after different times, were collected, centrifuged and washed two times with ice cold phosphate-buffered saline (PBS). The pellet was resuspended in lysis buffer. After the cells were lysed on ice for 30 min, lysates were centrifuged at $15000 \times g$ at 4 °C for 10 min. The protein concentration in the supernatant was determined using BCA protein assay reagents (Pierce, Italy). Equal amounts of protein (20 µg) were resolved using sodium dodecyl sulfate polyacrylamide gel electrophoresis (SDS–PAGE) (7.5–15% acrylamide gels) and transferred to a PVDF Hybond-p membrane (GE Healthcare). Membranes were blocked with I-block (Tropix), the membrane being gently rotated overnight at 4 °C. Membranes were incubated with primary antibodies against, Bcl-2, Mcl-1, Xiap, cleaved caspase-8, procaspase-2, PARP, cdc25C, Bax, survivin Thr34 and cdc2 (Tyr 15) (all rabbit, Cell Signalling, Milano, Italy), cyclin B1 (mouse, BD, Milano, Italy) cleaved caspase-3 (mouse, Alexis) or β-actin (mouse, Sigma–Aldrich, Milano, Italy) for 2 h at room temperature. Membranes were next incubated with peroxidase-labeled goat anti-rabbit IgG (Sigma–Aldrich, Milano, Italy) or peroxidase-labeled goat anti-mouse IgG (Sigma–Aldrich) for 60 min. All membranes were visualized using ECL Advance (GE Healthcare) and exposed to Hyperfilm MP (GE Healthcare). To ensure equal protein loading, each membrane was stripped and reprobed with anti-β-actin antibody.

Acknowledgment

The authors would like to thank Dr. Alberto Casolari for excellent technical assistance.

Supplementary data

Supplementary data associated with this article can be found, in the online version, at <http://dx.doi.org/10.1016/j.bmc.2012.10.001>.

References and notes

- (a) Honore, S.; Pasquier, E.; Braguer, D. *Cell. Mol. Life Sci.* **2005**, *62*, 3039; (b) Amos, L. A. *Org. Biomol. Chem.* **2004**, *2*, 2153.
- (a) Dumontet, C.; Jordan, M. A. *Nat. Rev. Drug Disc.* **2010**, *9*, 790; (b) Risinger, A. L.; Giles, F. J.; Mooberry, S. L. *Cancer Treat. Rev.* **2008**, *35*, 255; (c) Hearn, B. R.; Shaw, S. J.; Myles, D. C. *Compr. Med. Chem. II* **2007**, *7*, 81.
- (a) Yue, Q.-X.; Liu, X.; Guo, D.-A. *Planta Med.* **2010**, *76*, 1037; (b) Kingston, D. G. *J. Nat. Prod.* **2009**, *72*, 507.
- Pettit, G. R.; Singh, S. B.; Hamel, E.; Lin, C. M.; Alberts, D. S.; Garcia-Kendall, D. *Experientia* **1989**, *45*, 209.
- Lin, C. M.; Ho, H. H.; Pettit, G. R.; Hamel, E. *Biochemistry* **1989**, *28*, 6984.
- McGown, A. T.; Fox, B. W. *Cancer Chemother. Pharmacol.* **1990**, *26*, 79.
- Pettit, G. R.; Temple, C., Jr.; Narayanan, V. L.; Varma, R.; Boyd, M. R.; Renner, G. A.; Bansal, N. *Anti-Cancer Drug Des.* **1995**, *10*, 299.
- (a) Rustin, G. J.; Shreeves, G.; Nathan, P. D.; Gaya, A.; Ganesan, T. S.; Wang, D.; Boxall, J.; Poupard, L.; Chaplin, D. J.; Stratford, M. R. L.; Balkissoon, J.; Zweifel, M. *Br. J. Cancer* **2010**, *102*, 1355; (b) Siemann, D. W.; Chaplin, D. J.; Walike, P. A. *Expert Opin. Investig. Drugs* **2009**, *18*, 189.
- Tron, G. C.; Pirali, T.; Sorba, G.; Pagliai, F.; Busacca, S.; Genazzani, A. A. *J. Med. Chem.* **2006**, *49*, 3033.
- (a) Nam, N. H. *Curr. Med. Chem.* **2003**, *10*, 1697; (b) Cushman, M.; Nagarathnam, D.; Gopal, D.; He, H.-M.; Lin, C. M.; Hamel, E. *J. Med. Chem.* **1992**, *35*, 2293; (c) Hatanaka, T.; Fujita, K.; Ohsumi, K.; Nakagawa, R.; Fukuda, Y.; Nihei, Y.; Suga, Y.; Akiyama, Y.; Tsuji, T. *Bioorg. Med. Chem. Lett.* **1998**, *8*, 3371.
- (a) Chaudari, A.; Pandeya, S. N.; Kumar, P.; Sharma, P. P.; Gupta, S.; Soni, N.; Verma, K. K.; Bhardwaj, G. *Mini-Rev. Med. Chem.* **2007**, *12*, 1186; (b) Hsieh, H. P.; Liou, J. P.; Mahindroo, N. *Curr. Pharm. Des.* **2005**, *11*, 1655.
- Romagnoli, R.; Baraldi, P. G.; Brancale, A.; Ricci, A.; Hamel, E.; Bortolozzi, R.; Basso, G.; Viola, G. *J. Med. Chem.* **2011**, *54*, 5144.
- Brown, M. D.; Gillon, D. W.; Meakins, G. D.; Whitham, G. H. *J. Chem. Soc., Perkin. Trans. I* **1985**, 1623.
- Dall'Acqua, F.; Linardi, M. A.; Maggi, F.; Nicoletti, M.; Petitto, V.; Innocenti, G.; Basso, G.; Viola, G. *Bioorg. Med. Chem.* **2011**, *19*, 5876.
- Toffoli, G.; Viel, A.; Tuimoto, I.; Bisconti, G.; Rossi, G.; Baiocchi, M. *Br. J. Cancer* **1991**, *63*, 51.
- Dupuis, M.; Flego, M.; Molinari, A.; Cianfriglia, M. *HIV Med.* **2003**, *4*, 338.
- Martello, L. A.; Verdier-Pinard, P.; Shen, H. J.; He, L.; Torres, K.; Orr, G. A.; Horwitz, S. B. *Cancer Res.* **2003**, *63*, 448.
- Hamel, E. *Cell Biochem. Biophys.* **2003**, *38*, 1.
- Verdier-Pinard, P.; Lai, J.-Y.; Yoo, H.-D.; Yu, J.; Marquez, B.; Nagle, D. G.; Nambu, M.; White, J. D.; Falck, J. R.; Gerwick, W. H.; Day, B. W.; Hamel, E. *Mol. Pharmacol.* **1998**, *53*, 62.
- (a) Mollinedo, F.; Gajate, C. *Apoptosis* **2003**, *8*, 413; (b) Clarke, P. R.; Allan, L. A. *Trends Cell Biol.* **2009**, *19*, 89.
- Vakifahmetoglu-Norberg, H.; Zhivotovsky, B. *Trends Cell Biol.* **2010**, *20*, 150.
- Mhaidat, N. M.; Wang, Y.; Kiejda, K. A.; Zang, X. D.; Hersey, P. *Mol. Cancer Ther.* **2007**, *6*, 752.
- Ho, L. H.; Read, S. H.; Dorstyn, L.; Lambrusco, L.; Kumar, S. *Oncogene* **2008**, *27*, 3393.
- Bhalla, K. N. *Oncogene* **2003**, *22*, 9075.
- Wertz, I. E.; Kusam, S.; Lam, C.; Okamoto, T.; Sandoval, W.; Anderson, D. J., et al. *Nature* **2011**, *471*, 110.
- Matson, D. R.; Stukenberg, P. T. *Mol. Interv.* **2011**, *11*, 141.
- Altieri, D. C. *Biochem. J.* **2010**, *430*, 199.
- Castedo, M.; Perfettini, J. L.; Roumier, T.; Andreau, K.; Medema, R.; Kroemer, G. *Oncogene* **2004**, *23*, 2825.
- O'Connor, D. S.; Grossman, D.; Plescia, J.; Li, F.; Zhang, H.; Villa, A.; Tognin, S.; Marchisio, P. C.; Altieri, D. C. *Proc. Natl. Acad. Sci. U.S.A.* **2000**, *9*, 13103.
- Viola, G.; Fortunato, E.; Ceconet, L.; Del Giudice, L.; Dall'Acqua, F.; Basso, G. *Toxicol. Appl. Pharm.* **2008**, *227*, 84.
- Ravelli, R. B. G.; Gigant, B.; Curmi, P. A.; Jourdain, I.; Lachkar, S.; Sobel, A.; Knossow, M. *Nature* **2004**, *428*, 198.
- Molecular Operating Environment (MOE 2010), Chemical Computing Group, Inc. Montreal, Quebec, Canada. <http://www.chemcomp.com> (accessed Sep 2012).
- Korb, O.; Stützel, T.; Exner, T. E. *LNCS* **2006**, *4150*, 247.
- Case, D. A.; Cheatham, T. E., III; Darden, T.; Gohlke, H.; Luo, R.; Merz, K. M., Jr.; Onufriev, A.; Simmerling, C.; Wang, C.; Woods, R. J. *Comput. Chem.* **2005**, *26*, 1668.
- Humphrey, W.; Dalke, A.; Schulten, K. *J. Mol. Graph.* **1996**, *14*, 33.